Asian Journal of Chemistry; Vol. 25, No. 15 (2013), 8810-8816

ASIAN JOURNAL OF CHEMISTRY

http://dx.doi.org/10.14233/ajchem.2013.15777

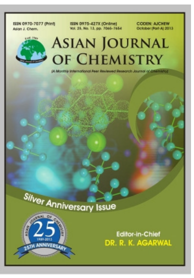

Chemical Effects of CO_2 Concentration on Flame Structure and Soot Precursors in Rich Ethylene Oxidation

YINDI ZHANG[1,2,*], CHUN LOU[2,*] and YONG LI[3]

[1]Yangtze University Research for China National Petroleum Corporation Key Laboratory of Oil Gas Production, Wuhan 430100, Hubei Province, P.R. China
[2]State Key Laboratory of Coal Combustion, Huazhong University of Science and Technology, Wuhan 430074, Hubei Province, P.R. China
[3]Gas Lift Technology Center of Tuha Oilfield of China National Petroleum Corporation, Hami 838202, Xinjiang Province, P.R. China

*Corresponding authors: Tel: +86 18 971693567; E-mail: yindi.zhanghust@gmail.com; ChunLou@mail.hust.edu.cn

(*Received*: 15 May 2013; *Accepted*: 29 August 2013) AJC-14054

Flame structure and soot precursors were investigated numerically with CO_2 addition in fuel enrichment laminar premixed $C_2H_4/O_2/Ar$ flames (C/O ratio of $\Phi = 2.5$) at low pressure (0.05 atm). An updated mechanism emphasizes the effect of presence of an O_2/CO_2 atmosphere instead of an O_2/Ar one in premixed flame. The addition of CO_2 in the fresh gas inlet causes a shift downstream of the flame front and thus flame inhibition. The partial replacement of Ar by CO_2 leads to an increase of burnt gas quantities of H_2O, CO and CO_2 and leads to a decrease of the maximum mole fractions of some C_2 to C_{10} hydrocarbon intermediates (C_2H_2, C_3H_3, C_6H_6, C_6H_6O, C_8H_8 and $C_{10}H_8$). The sensitivity analysis and reaction-path analysis show that C_2H_4 reaction path and products are altered due to the CO_2 addition.

Key Words: Fuel enrichment, Carbon dioxide, Kinetics modeling, Flame structure, Soot precursors.

INTRODUCTION

Exhaust gas recirculation systems and oxy-fuel burners with CO_2 recycling have been used successfully in a number of industrial processes and shown to improve combustion efficiency and reduce pollutant emissions. However, these industrial processes are mostly accompanied by NOx and soot particles emission which have a detrimental effect on human health and contribute significantly to global warming[1-3]. So, the radiative properties of oxy-fuel flames and the role of soot is a persistent problem in many processes that involve fuel-rich combustion of hydrocarbon fuels[4].

A number of investigations have been focused on reducing soot emission by introducing several techniques, including the use of different fuels and addition of diluents on the oxidizer or fuel side in diffusion flames. Especially, study of the effect of CO_2 additives on soot emission has been a special interest for suppressing soot production tendency, such as those by Ni and co-workers[5] and Liu and co-workers[6]. These investigations found that the addition of CO_2 on either fuel side or oxidizer has chemical effects on soot formation reduction, which might be to promote the concentrations of oxygen atom and hydroxyl that in return increase the oxidation of soot precursors in soot formation regions, in addition to dilution and thermal effects.

Recently two experimental investigations have been co nducted by Renard *et al.*[7] and Vandooren *et al.*[8] on CO_2 addition to rich $C_2H_4/O_2/Ar$ and $CH_4/O_2/Ar$ premixed flames. The results showed that CO_2 and H_2O addition are responsible for reduction of hydrocarbon intermediates in flames. It has been established experimentally that addition of CO_2 suppresses soot emission chemically in both diffusion and premixed flames. However, the chemical effects of CO_2 addition on flame structure in premixed flames remains unclear, especially for computation investigation.

The main objective of this study is to numerically investigate the mechanism of the chemical effect of CO_2 addition on the structure of premixed rich $C_2H_4/O_2/Ar(N_2)$ flames at low pressure and atmospheric pressure. An updated mechanism of C_2H_4/air combustion based on Kazakov *et al.*[3] with emphasis on CO_2 addition was modified from previous studies in the literature. The main combustion concentration profiles have been predicted using the updated mechanism and verified against the experimental data. The test conditions were limited to fuel-rich laminar premixed ethylene/air flames at low pressure and different C/O ratios, similar to the flames studied by Renard[7] and Vandoorens[8]. To further understand the effect of CO_2 addition on soot formation at atmospheric pressure. The kinetic models were scrutinized with sensitivity, rate of production analysis and path of reaction analysis.

Combustion mechanisms and simulation

Reaction mechanism without CO_2 additive: In this article, the gas-phase original comprehensive reaction mechanism was developed by Kazakov and co-workers[3] for the oxidation of C_2H_4 in air combustion. The detailed chemical kinetic model consisted of 680 reactions and 156 species. Calculation was performed using the Premixed Laminar Model of the CHEMKIN-PRO package. Thermodynamic properties were obtained from CHEMIKIN database. Transport properties were obtained from the Sandia CHEMIKIN transport data base[9]. Some species were predicted and verified against the experimental data in premixed $C_2H_4/O_2/Ar$ without CO_2 addition at low pressure.

The main species involving soot precursors are discussed in detail, such as reactants, products, acetylene, benzene, pyrene and so on. The role of resonantly stabilized radicals were investigated in aromatic, branched aromatic and polycyclic aromatic hydrocarbon formation in a premixed, rich, laminar, $C_2H_4/O_2/Ar$ flame.

Reaction mechanism with CO_2 additive: The computed results on polycyclic aromatic hydrocarbon formation for C_2H_4 oxidation in different O_2/CO_2 atmospheres are analyzed in terms of a gas-phase chemical kinetic model, which was updated from the mechanism of Kazakov and co-workers[3]. This mechanism provides in general reasonably good agreement between modeling and experimental results, even though some modifications are needed to take into account the effect of the presence of high CO_2 concentration levels. An updated mechanism was developed to identify the chemical effects of an additive (CO_2) introduced to the fuel mixture. Therefore, in the present work, the mechanism has been updated, with particular emphasis on the effect of the presence of an O_2/CO_2 atmosphere instead of air or O_2/Ar. A number of reactions involving CO_2 species which do not appear in the initial model but may be important during the C_2H_4 oxidation process under oxy-fuel conditions have been included. Moreover, revisions of rate constants of the most sensitive reactions in the mechanism under the specific conditions studied were modified based on previous studies in the literature. These modifications and the main reactions of interest are performed as an attempt to attain a better prediction of the experimental data. The modifications are listed in Table-1. These modifications and the main reactions of interest are described below. Calculations are performed using the PREMIX model. The reverse rate constants were taken from the same source as the mechanism.

In order to establish the reaction mechanism, the conversion of CO_2 to CO (Table-1) needs to be emphasized for activating chemically the comparatively inert CO_2 molecule. The strong carbon-oxygen double bonds in CO_2 need to spend high temperature or very reactive free radical breaking it.

The reaction of thermal dissociation for CO_2

$$CO + O(+M) \rightleftharpoons CO_2(+M) \tag{R1}$$

which occurs only at high temperatures with strongly endothermic. The most important reaction with atomic hydrogen

$$CO_2 + H \rightleftharpoons CO + OH \tag{R2}$$

is comparatively fast even at medium temperatures. This reaction would be the dominating reaction under combustion conditions for CO/CO_2 partial equilibrium. The rate constant for the reaction can be seen in[10-19].

Reactions of other species with CO_2 from the O/H radical pool, *i.e.*:

$$CO_2 + OH \rightleftharpoons CO + HO_2 \tag{R4}$$

$$CO_2 + O \rightleftharpoons CO + O_2 \tag{R5}$$

are important because of slow.

The most abundant intermediate radical species is CH_3 for C_2H_4 combustion. The CH_3 may react with CO_2 to form CH_3O and CO

$$CH_3 + CO_2 \rightleftharpoons CH_3O + CO \tag{R11}$$

which reaction for the reverse direction, $CH_3O + CO \rightleftharpoons CH_3 + CO_2$ (R11), shows little consistency[20] with available results. Wang *et al.*[21] study results show that addition/elimination to $CH_3 + CO_2$ and direct H atom abstraction to $CH_2O + HCO$ is important at higher temperatures. The overall rate constant which was calculated by Wang *et al.*[21] indicates that lies above the low-temperature results of Koch *et al.*[22] and below those of Wantuck *et al.*[23] at high temperatures. According to Rasmussen and Glarborg[14], $CH_3 + CO_2$ is the sole product channel from $CH_3O + CO$ and the result was adopted [24].

TABLE-1
REACTIONS SUBSET FOR CO_2

	Reactions	A [cm, mol, s]	β	E_a [cal/mol]	Ref.
1	$CO+O(+M)\rightleftharpoons CO_2(+M^a)$	1.8×10^{10}	0	2384	10,11
	Low-pressure limit:	1.4×10^{24}	-2.79	4191	11,12
2^b	$CO+OH\leftrightarrows CO_2+H$	8.0×10^{10}	0	0	13
		8.8×10^{5}	1.77	954	
3	$CO+OH\leftrightarrows HOCO$	2.0×10^{16}	-5.6	2881	13
4	$CO+HO_2\rightleftharpoons CO_2+OH$	1.0×10^{5}	2.18	179400	14
5	$CO+O_2\rightleftharpoons CO_2+O$	4.7×10^{12}	0	60500	15
6	$HOCO\rightleftharpoons CO_3+H$	3.5×10^{56}	-15	46500	13
		2.5×10^{69}	-18	60000	
7^b	$HOCO+OH\leftrightarrows CO_2+H_2O$	4.6×10^{12}	0	-89	16
		9.5×10^{6}	2	-89	
8	$HOCO+OH\rightleftharpoons CO_2+HO_2$	9.9×10^{11}	0	0	17
9	$HCO+O\rightleftharpoons CO_2+H$	3.0×10^{13}	0	0	18
10	$HCO+HO_2\rightleftharpoons CO_2+OH+H$	3.0×10^{13}	0	0	19
11	$CH_3O+CO\leftrightarrows CH_3+CO_2$	9.5×10^{25}	-4.93	9080	20
12	$^3CH_2+CO_2\rightleftharpoons CH_2O+CO$	1.0×10^{11}	0	1000	21
13	$^1CH_2+CO_2\rightleftharpoons CH_2O+CO$	1.1×10^{13}	0	0	22
14	$CH+CO_2\leftrightarrows HCO+CO$	8.8×10^{6}	1.75	-1040	28

[a]Enhanced third-body efficiencies: $H_2 = 2.5$, $H_2O = 12$, $CO = 1.9$, $CO_2 = 3.8$.[b]Expressed as the sum of the constants.

Reactions of CO_2 with small hydrocarbon fragments include

$$^3CH_2 + CO_2 \rightleftharpoons CH_2O+CO \quad (R12)$$

$$^1CH_2 + CO_2 \rightleftharpoons CH_2O+CO \quad (R13)$$

$$CH + CO_2 \rightleftharpoons HCO+CO \quad (R14)$$

$$C+CO_2 \rightleftharpoons CO+CO$$

The CH_2 radical has two existing states in combustion processes. Singlet methylene ($^3CH_2$) is more reactive toward radicals than the triplet state ($^1CH_2$), but its reacts slower with stable molecules.

The measurement results show that reaction R12 is less than an order of magnitude slower reaction R13 (Table-1), but they are uncertain for the rate constants of these reactions.

The rate constant used for $^3CH_2 + CO_2$ relies on the room temperature measurement by Laufer and Bass[24] and the activation energy was assessed in the present work. Nevertheless, the most research results indicate that the reaction may be even slower in room temperature. For $^1CH_2 + CO_2$ (R13), the early estimate by Tsang and Hampson[19] under the room temperature shows a somewhat slower rate constant than the only experimental value by Koch *et al.*[22].

In this paper, the data obtained from those research data and reasonable estimates for Arrhenius expression shown in Table-1.

The model assumes that nucleation of soot particles is due to the coalescence of two large size polycyclic aromatic hydrocarbon, pyrene (A4), into a dimer. Then the particle size increases or decreases due to the particle coagulation, surface growth and oxidation.

EXPERIMENTAL

First of all, the experimental data for three premixed flames at equivalence ratios in the range of 1.00-2.00 (1.00, 1.50 and 2.00) are obtained from Renard *et al.*[25] to validate the original model on a flame burner 8 cm in diameter at pressures varying from 0.03 to 0.05 atm. In addition, the experimental data of rich premixed $C_2H_4/O_2/Ar$ flames for one without any additive (F2.50) and one with 15 % of CO_2 replacing the same quantity of argon (F2.50C) were obtained (Renard *et al.* [7] and Ho and Chou[26] to investigate the effect of CO_2 on the premixed flame of C_2H_4). The mole detail about experimental data can be seen in Table-2.

RESULTS AND DISCUSSION

Without CO_2 addition in premixed $C_2H_4/O_2/Ar$ flames: The simulations were performed for three premixed flames at equivalence ratios in the range of 1.0-2.0 (1.0, 1.5 and 2.0) to test the original model on a flame burner 8 cm in diameter at pressures varying from 0.03-0.05 atm (Table-2). The simulations of experimental data from Renard *et al.*[25], the molecular beam mass spectrometry (MBMS) measurements of species in a fuel-rich $C_2H_4/O_2/Ar$ flame, are presented in Fig. 1. The predicted and experimental mole fraction of C_2H_4 and H_2 concentrations are shown in Fig. 1(a-b). The simulated concentrations of small molecules and radicals H_2 and C_2H_4 are in good agreement with the experimental data. In general, the maximum error of C_2H_4 and H_2 concentrations for three equivalence ratios are under-predicted by 13.3 %. In view of systematic errors in the measurement, this under-prediction can be accepted.

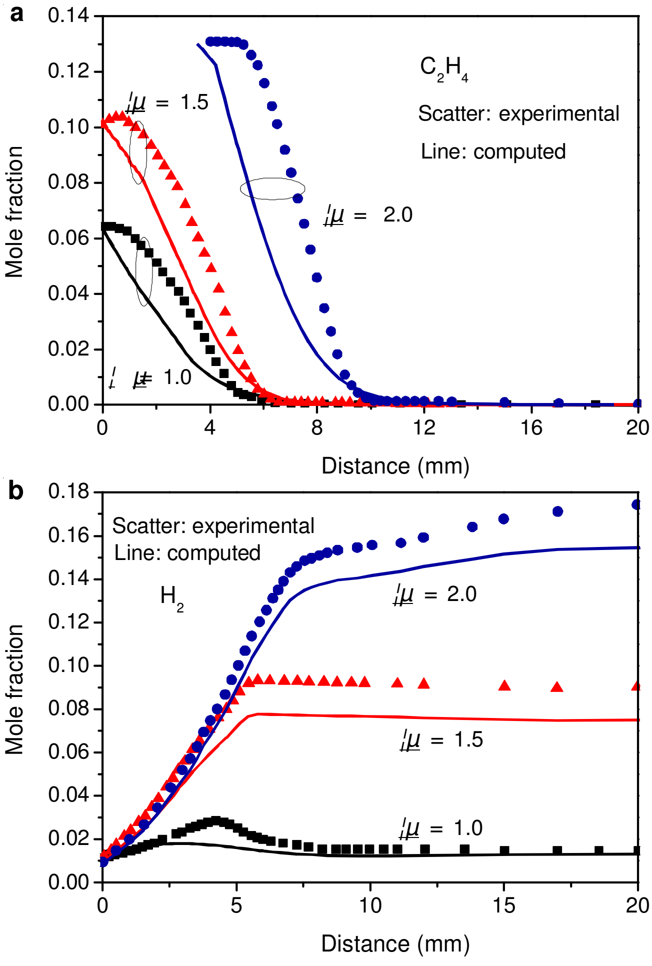

Fig. 1. Comparison of model predictions with experimental concentration profiles in the $C_2H_4/O_2/Ar$ flame for various several equivalence ratio (Φ). (a) Comparison for C_2H_4. (b) Comparison for H_2

Effect of CO_2 addition in premixed $C_2H_4/O_2/CO_2/Ar$ flames: The computed results on polycyclic aromatic hydrocarbon formation for C_2H_4 oxidation in various $O_2/CO_2/Ar$ atmospheres are analyzed in terms of a detailed gas-phase

TABLE-2
FLAME COMPOSITION AND COMPUTED CONDITIONS

Model	Flames	Φ	$X(C_2H_4)$	$X(O_2)$	X(Ar)	$X(CO_2)$	P (atm)	v_0 (cm/s)
Premix model	F1.0	1.0	0.0675	0.2025	0.7300	0	0.03	78.36
	F1.5	1.5	0.1012	0.2025	0.6963	0	0.04	58.79
	F2.0	2.0	0.1350	0.2025	0.6625	0	0.05	47.03
	F2.5	2.5	0.3300	0.4000	0.2700	0	0.05	40.3
	F2.5C	2.5	0.3300	0.4000	0.1200	0.1500	0.05	40.3

chemical kinetic model. The comprehensive reaction mechanism used as the starting mechanism for the modeling study was developed by Kazakov and co-workers[3] for the oxidation of C_2H_4 in air combustion. An updated mechanism was developed to identify the chemical effects of an additive (CO_2) introduced to the fuel mixture. Therefore, the updated mechanism emphasizes the effect of the presence of an O_2/CO_2 atmosphere instead of air or O_2/Ar. The modifications are listed in Table-1. Calculations were performed using the PREMIX model. The reverse rate constants were taken from the same source as the mechanism. In this section, only temperature and mole fraction profiles of important species involving soot formation are discussed in detail.

The addition of CO_2 replacing an equivalent amount of argon (Table-2) to the rich ethylene flame F2.5 has led to several effects which are described below. The simulated and experimental temperature and mole fraction profiles of H_2O in F2.5 and F2.5C flames are shown in Fig. 2. The simulated results agree well with the experimental data, even if the predictions of temperature and H_2O mole fraction are a little higher than the experimental results for both F2.5 and F2.5C. According to Renard and co-workers [25], the difference is due to experimental uncertainties. Indeed, the replacement of some quantities of argon by equivalent amounts of CO_2 leads to a displacement of the flame front of 1-2 mm downwards and to an increase in the mean heat capacity. The partial replacement of Ar by CO_2 leads to an increase of burnt gases quantities of H_2O, CO and CO_2.

As it is illustrated in Figs. 2b and 3a, the presence of CO_2 in the fresh gases (F2.50C) induces larger yields of CO (17 %) and H_2O (25 %) through the overall reaction

$$CO_2 + H_2 \rightleftharpoons CO + H_2O$$

For the doped flame (F2.50C), a decrease of the burning velocities was observed compared to the F2.50 flame, which consists of a shift of the flame front about 0.5-1.0 mm downstream from the burner surface as is easily observed through the mole fraction profiles of C_2H_4 (Fig. 3b). From Fig. 3b, the presence of CO_2 in the fresh gases (F2.50C) induces an increase of final quantities of CO_2 (37 %). Also, the simulated profiles of CO, CO_2, C_2H_2 and C_2H_4 agree well with the experimental ones (Fig. 3).

Fig. 4 shows the maximum mole fractions of some C_2 to C_{10} species at equivalence ratio of 2.50. The simulated results agree well with the experimental data, even if the prediction of C_6H_6O is a little higher than the experimental result. CO_2 addition usually leads to a decrease by only about 5-20 % of the maximum mole fractions of some C_2 to C_{10} hydrocarbon intermediates (C_2H_2, C_3H_3, C_6H_6, C_6H_6O, C_8H_8 and $C_{10}H_8$) (Figs. 3b and 4). The decrease of that of C_2H_2 is more marked in the flame F2.50C (30 %).

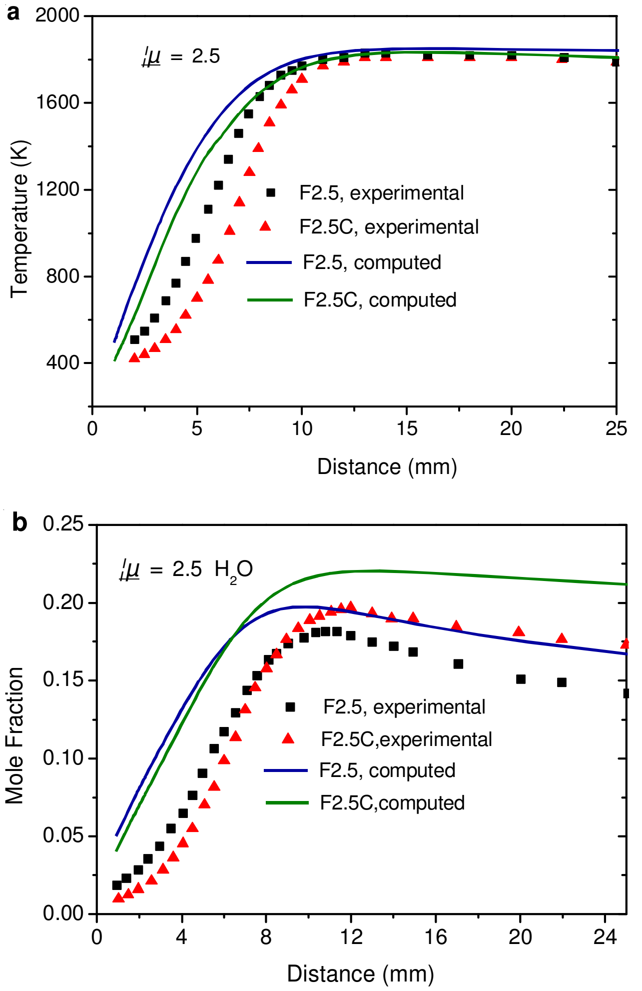

Fig. 2. Comparison of predicted profiles with the experimental profiles in the C_2H_4/O_2/Ar and $C_2H_4/O_2/Ar/CO_2$ flames at Φ = 2.5. (a) Comparison for temperature. (b) Comparison for H_2O

Sensitivity analysis and reaction path analysis: The $C_2H_4/O_2/Ar(N_2)$ combustion mechanism of Kazakov and co-workers [3] is used in the simulation. This reaction mechanism consists of 156 species and 680 reactions which include polycyclic aromatic hydrocarbon growth reactions up to pyrene, A4. The code names for some are shown in Table-3. According to Frenklach and co-workers[10], soot particles are created by the dimerization of pyrene molecules.

TABLE-3
AROMATIC SPECIES

No.	Name	Structure	No.	Name	Structure
1	Phenyl, A1-	C_6H_5	11	Naphthalene, A2	$C_{10}H_8$
2	Benzene, A1	C_6H_6	12	Biphenyl, P2	$C_{12}H_{10}$
3	Toluene	C_7H_8	13	Methylnaphthalene, A2CH_3	$C_{11}H_{10}$
4	Benzyl, C_7H_7	$C_6H_5CH_2$	14	Ethynylnaphthalene, A2C_2H	$C_{12}H_8$
5	Phenyl acetylene, A1C_2H	$C_6H_5C_2H$	15	Acenaphthalene, A2R5	$C_{12}H_8$
6	Ethynylphenyl radical, A1C_2H-	C_6H_4CCH	16	Phenanthrene, A3	$C_{14}H_{10}$
7	Styrene, A1C_2H_3	$C_6H_5C_2H_3$	17	Methylphenanthrene	$C_{14}H_{12}$
8	Phenylvinyl radical, A1C_2H_3*	$C_6H_4CH=CH_2$	18	Phenanthrylacetylen, A3C_2H	$C_{16}H_{10}$
9	*n*-Styryl, *n*-C_8H_7	$C_6H_5CH=CH$	19	Pyrene, A4	$C_{16}H_{10}$
10	Indene	C_9H_8	20	Pyreneacetylene, A4C_2H	$C_{18}H_{10}$

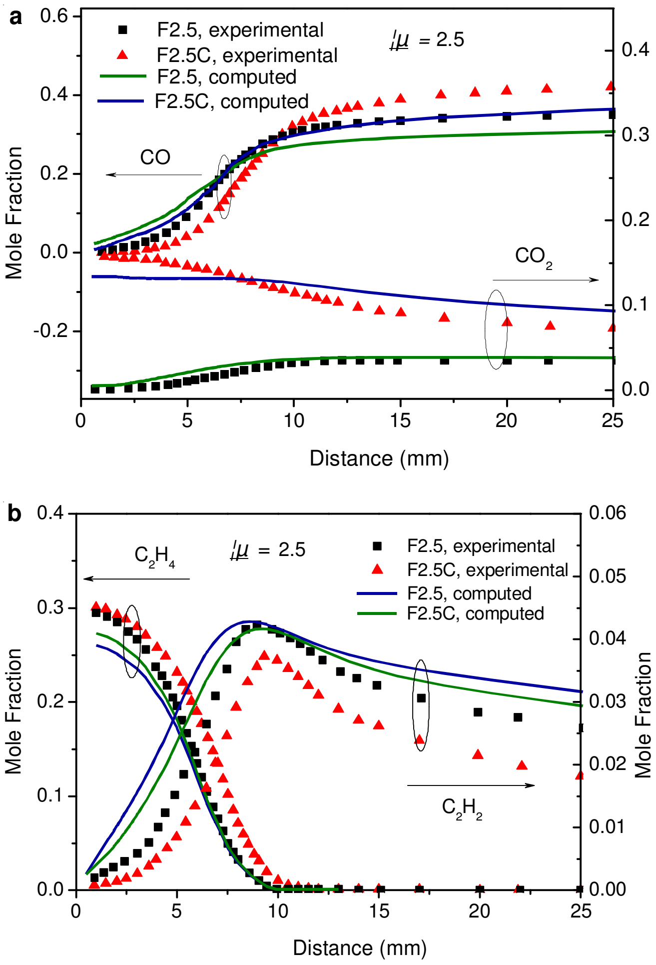

Fig. 3. Comparison of predicted mole profiles of main C_1-, C_2-species with the experimental profiles in the $C_2H_4/O_2/Ar$ and $C_2H_4/O_2/Ar/CO_2$ flames at $\Phi = 2.5$. (a) Comparison for CO_2 and CO. (b) Comparison for C_2H_4 and C_2H_2

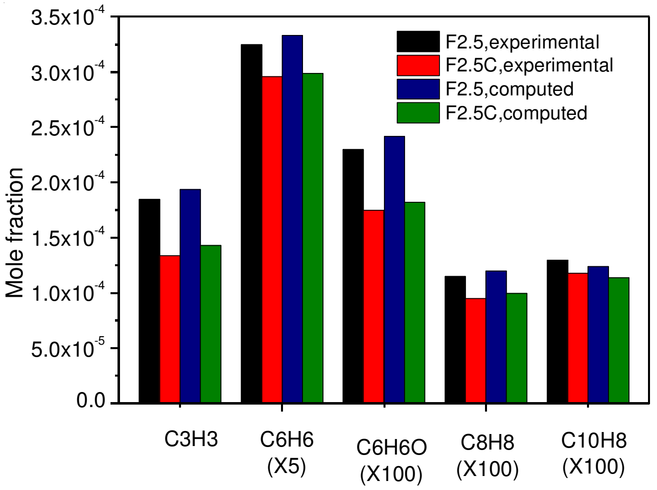

Fig. 4. Comparison of maximum prediction of mole profiles of main C_3-C_{10} species (C_3H_3, C_6H_6, C_6H_6O, C_8H_8 and $C_{10}H_8$) with the experimental profiles in the $C_2H_4/O_2/Ar$ and $C_2H_4/O_2/Ar/CO_2$ flames at $\Phi = 2.5$

According to the mechanism (Fig. 5a), the most important consumption reaction of ethylene is $C_2H_4 + H = C_2H_3 + H_2$ which is the main route for the formation of vinyl radicals. This C_2H_3 radical leads to the formation of acetylene (C_2H_2) by decomposition. Acetylene is an important compound since it has been recognized as an important precursor for soot formation. Indeed, C_2H_2 allows the formation of C_3 and C_4 hydrocarbons. The main formation of propargyl radicals comes from the reaction of acetylene with singlet methylene radicals: $C_2H_2 + {}^1CH_2 = C_3H_3 + H$. Moreover, C_3H_3 can be produced from propyne and allene by hydrogen abstraction. The combination of resonantly stabilized free radicals such as propargyl, allyl, 1-methylallenyl and cyclopentadienyl were identified as an important aromatic and polycyclic aromatic hydrocarbon precursor species which eventually lead to benzene, toluene, xylene, naphthalene and phenanthrene formation in flames. These resonantly stabilized radicals play an important role in aromatic and polycyclic aromatic hydrocarbon formation as these species can build up in concentration within the flame since they are relatively resistant to oxidation by O_2.

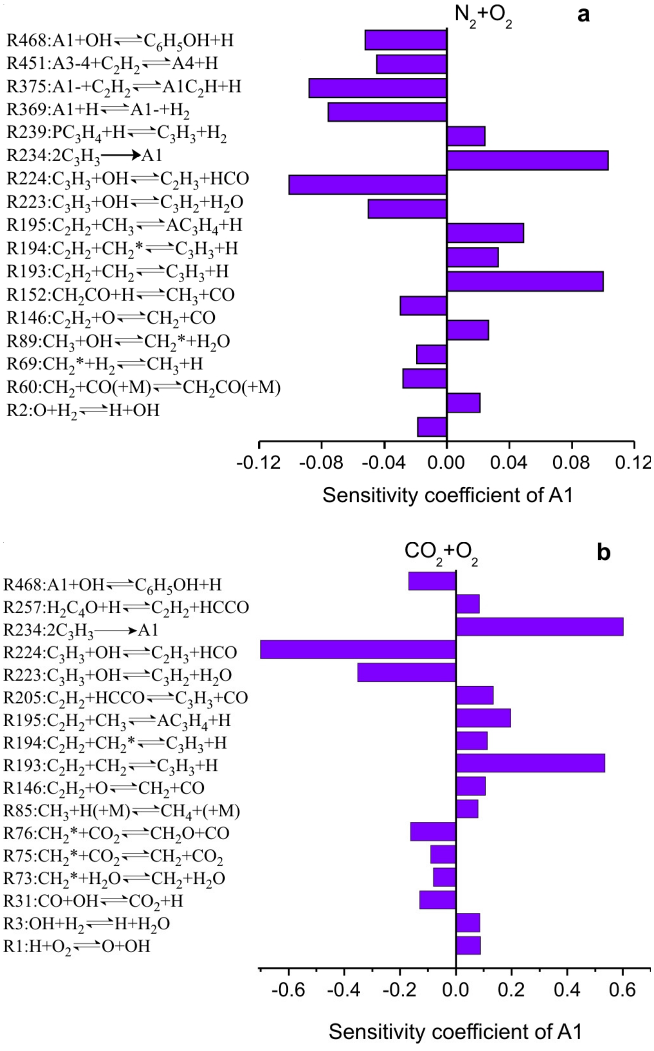

Fig. 5. Comparison of sensitivity analysis without and with CO_2 additive in the $C_2H_4/O_2/N_2$ flames at $\Phi = 2.2$

The important steps in soot formation from gas phase hydrocarbons are believed to be formation of the first ring, formation of polycyclic aromatic hydrocarbons (PAHs), soot inception and subsequently soot growth. It is now widely accepted that benzene and phenyl formation constitutes the first step in this growth process that lead to polycyclic aromatic hydrocarbon and ultimately soot particles. However, despite the extensive work on the elementary reactions leading to the first aromatic ring, neither the dominant benzene (C_6H_6, A1) formation pathway nor the sensitivity of benzene (C_6H_6, A1) in $C_2H_4/O_2/N_2$ and $C_2H_4/O_2/CO_2$ atmosphere is yet well understood.

Fig. 5 shows the results of C_6H_6 (A1) normalized sensitivity coefficients of 17 reactions for $C_2H_4/O_2/N_2$ (Fig. 5a) and $C_2H_4/O_2/CO_2$ (Fig. 5b) flames at 1 atm and temperature 1630 K. There are three reactions (R234, R224 and R193) at 1630 K:

$2C_3H_3 \Rightarrow A1$ R234

$C_3H_3+OH \Leftrightarrow C_2H_3+HCO$ R224

$C_2H_2+CH_2 \Leftrightarrow C_3H_3+H$ R193

which have absolute values of sensitivity coefficients that are larger in both flames. However, there are some reactions that are different in the two flames; such as R451, R375, R239, R369, R152, R89, R69, R60 and R2. These nine reactions appear in Fig. 5a but are replaced by R257, R205, R85, R76, R75, R73, R31, R3 and R1 in Fig. 5b. So, the C_2H_4 oxidation is changed due to CO_2 addition. Some reactions that have higher sensitivity coefficients are not presented here.

Finally, the typical reaction-path diagrams in Fig. 6 represent the main reactions and species leading to benzene formation in $C_2H_4/O_2/N_2$ atmosphere (Fig. 6a) and $C_2H_4/O_2/CO_2$ atmosphere (Fig. 6b). Such diagrams, resulting from combining Fig. 5, are useful in identifying the difference in benzene formation in the different atmospheres. In Figs. 6a-b, the hydroxide radical (OH), oxygen radical (O) and other side species (H) are chosen as side species. Any reaction with the hydroxide radical is coloured purple, any reaction with the oxygen radical is coloured green and any reaction with H is coloured black. Each substantial reaction is represented by an arrow, the thickness of which is representative of the relative importance of that particular reaction of formation. The diagrams are not representative of all reactions in the mechanism but only concern the main pathways leading to benzene formation.

From Fig. 6, benzene formation is mainly achieved in two ways: $C_2H_2 \rightarrow C_3H_3 \rightarrow A1(C_6H_6)$ and $C_2H_2 \rightarrow A1(C_6H_6)$ in both $C_2H_4/O_2/N_2$ and $C_2H_4/O_2/CO_2$ atmosphere. From Fig. 6a, besides conversion of small amounts to CO, most of the C_3H_3 converts to A1 in $C_2H_4/O_2/N_2$ atmosphere. However, besides most of the C_3H_3 converting to A1 and CO, a certain amount of C_3H_3 converts to HCO in Fig. 6b. So, this is a factor that the soot volume fraction decreases in the $C_2H_4/O_2/CO_2$ flame compared to the $C_2H_4/O_2/N_2$ flame. Comparing Figs. 6a-b, there are different main paths between the two. They are $C_2H_4 \rightarrow C_2H_2 \rightarrow C_4H_2 \rightarrow$ i-$C_4H_2 \rightarrow CH_2CO \rightarrow CO_2$, $C_2H_4 \rightarrow C_2H_2 \rightarrow C_4H_2 \rightarrow$ i-$C_4H_2 \rightarrow CH_2CO \rightarrow CH_3 \rightarrow CH_4$ in the $C_2H_4/O_2/N_2$ flame (Fig. 6a) and $C_2H_4 \rightarrow C_2H_2 \rightarrow C_4H_2 \rightarrow H_2C_4O \rightarrow CH_2CO \rightarrow CH_3$ $CH_2O \rightarrow HCO$ in the $C_2H_4/O_2/N_2$ flame (Fig. 6b). It can be concluded that CO_2 in the atmosphere changed the path of C_2H_4 oxidation.

Conclusion

A kinetic modeling study was carried out to investigate the mechanism of the chemical effects of CO_2 addition on the flame structure in a premixed flame under a pressure of 0.05 atm at equivalence ratios $\Phi = 2.5$. An updated mechanism, which was applied and shown to reproduce reasonably well the concentration profiles of major, intermediate and aromatic species in ethylene flames, focused on the effect of the presence of an O_2/CO_2 atmosphere instead of air or O_2/Ar. Numerical results were verified against experimental data. Modeling predictions of reactants, stable intermediates and polycyclic aromatic hydrocarbon compounds generally showed good agreement with experimental data.

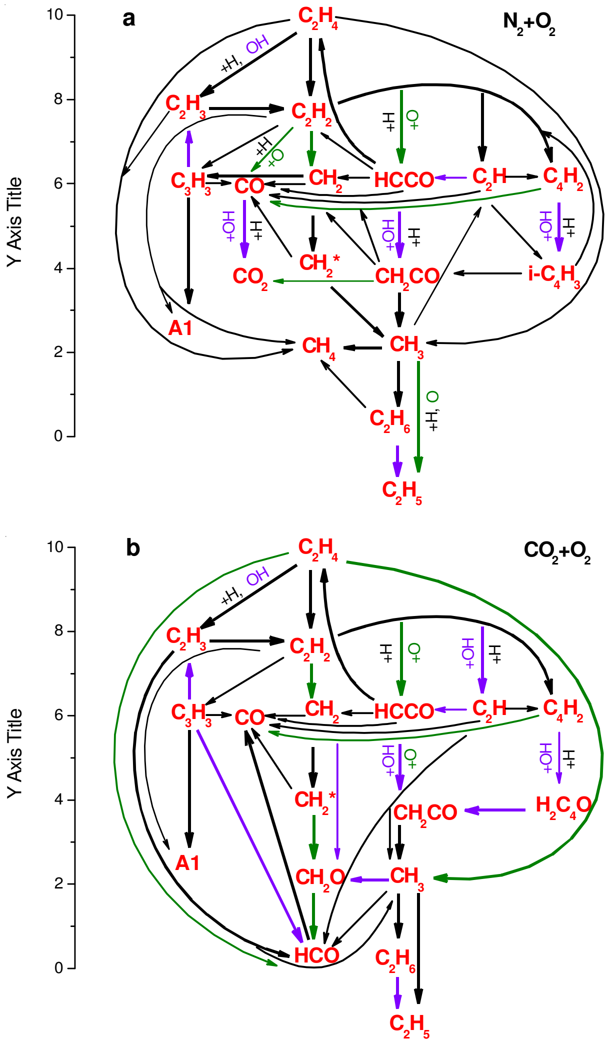

Fig. 6. Comparison of reaction analysis without and with CO_2 additive in the $C_2H_4/O_2/N_2$ flames at $\Phi = 2.2$

The addition of CO_2 in the fresh gas inlet causes a shift downstream of the flame front and thus flame inhibition, in the premixed $C_2H_4/O_2/CO_2$/Ar flame. The partial replacement of Ar by CO_2 leads to an increase in burnt gases quantities of H_2O, CO and CO_2 and leads to a decrease in the maximum mole fractions of some C_2 to C_{10} hydrocarbon intermediates (C_2H_2, C_3H_3, C_6H_6, C_6H_6O, C_8H_8 and $C_{10}H_8$).

The sensitivity analysis and reaction-path analysis were conducted for $C_2H_4/O_2/N_2$ and $C_2H_4/O_2/N_2/CO_2$. The results show that C_2H_4 reaction path and products are altered due to the CO_2 addition.

ACKNOWLEDGEMENTS

The authors gratefully expressed their thanks for the financial support for these researches from the Foundation of State Key Laboratory of Coal Combustion and from the National Natural Science Foundation of China (No. 51306022).

REFERENCES

1. C. Ce'cile, C. Christian, G.Ö. Iskender and F.K. Dilek, *Proc. Combust. Inst.*, **32**, 1803 (2009).
2. C.O. Kwang and D.S. Hyun, *Fuel*, **85**, 615 (2006).
3. A. Kazakov, H. Wang and M. Frenklach, *Combust. Flame*, **100**, 111 (1995).
4. M.S. Skjøth-Rasmussen, P. Glarborg, M. Østberg, J.T. Johannessen, H. Livbjerg, A.D. Jensen and T.S. Christensen, *Combust. Flame*, **136**, 91 (2004).
5. T. Ni, S.B. Gupta and R.J. Santoro, *Proc. Combust. Inst.*, **25**, 1379 (1994).
6. F. Liu, H. Guo, G.J. Smallwood and Ö. Gulder, *Combust. Flame*, **125**, 778 (2001).
7. C. Renard, V. Dias, P.J. van Tiggelen and J. Vandooren, *Proc. Combust. Inst.*, **32**, 631 (2009).
8. J. Vandooren, L. Thill, M. Musick and P.J. van Tiggelen, Paper Presented at the 20th Task Leaders Meeting of the IEA implementing agreement. Depletion of Soot Precursors by CO_2 Addition to Rich Hydrocarbon Flames, Energy Conservation and Emission Reduction in Combustion, Ottawa, Ont. July, pp. 26-29 (1998).
9. R.J. Kee, G. Dixon-Lewis, J. Warnatz, M.E. Coltrin and J.A. Miller, The Chemkin Transport Database. Sandia Report #SAND.86-8246. Sandia National Laboratories (1986).
10. M. Frenklach and H. Wang, In ed.: H. Bockhorn, Detailed Mechanism and Modeling of Soot Particle Formation. Springer Series in Chemical Physics. Springer-Verlag: Berlin, Vol. 59, 165 (1994).
11. J. Troe, *Proc. Combust. Inst.*, **15**, 667 (1975).
12. M.T. Allen, R.A. Yetter and F.L. Dryer, *Combust. Flame*, **109**, 449 (1997).
13. P.R. Westmoreland, J.B. Howard and J.P. Longwell, *AIChE J.,* **32**, 1971 (1986).
14. C.L. Rasmussen, J. Hansen, J. Marshall and P. Glarborg, *Int. J. Chem. Kinet.,* **40**, 454 (2008).
15. X. You, H. Wang, E. Goos, C.-J. Sung and S.J. Klippenstein, *J. Phys. Chem. A*, **111**, 4031 (2007).
16. H.-G. Yu, J.T. Muckerman and J.S. Francisco, *J. Phys. Chem. A*, **109**, 5230 (2005).
17. J. Nolte, J. Grussdorf, F. Temps and H.G. Wagner, *Z. Naturforsch.*, **48a**, 1234 (1993).
18. D.L. Baulch, C.T. Bowman, C.J. Cobos, R.A. Cox, Th. Just, J.A. Kerr, M.J. Pilling, D. Stocker, J. Troe, W. Tsang, R.W. Walker and J. Warnatz, *J. Phys. Chem. Ref. Data*, **34**, 757 (2005).
19. W. Tsang and R. Hampson, *J. Phys. Chem. Ref. Data*, **15**, 1087 (1986).
20. P. Glarborg, J.A. Miller and R.J. Kee, *Combust. Flame.* **65**, 177 (1986).
21. B. Wang, H. Hou and Y. Gu, *J. Phys. Chem. A*, **103**, 8021 (1999).
22. M. Koch, F. Temps, R. Wagener and H.Gg. Wagner, *Ber. Bunsenges. Phys. Chem.*, **94**, 645 (1990).
23. P.J. Wantuck, R.C. Oldenborg, S.L. Baughcum and K.R. Winn, *Chem. Phys. Chem.*, **91**, 3253 (1987).
24. A.H. Laufer and A.M. Bass, *Int. J. Chem. Kinet.*, **7**, 639 (2004).
25. C. Renard, M. Musick, P.J. Van Tiggelen and J. Vandooren, *Proc. Eur. Combust. Meet.*, **25**, 1 (2003).
26. P. Ho and C.-P. Chou, Reaction Design (2006).